EVALUATION OF ELECTRON BEAM WELDED JOINTS PROPERTIES OF ADDITIVELY MANUFACTURED AND CONVENTIONAL ALUMINIUM ALLOYS

RADOSLAV VANDZURA[1], MATUS GELATKO[1], MICHAL HATALA[1], FRANTISEK BOTKO[1], SVETLANA RADCHENKO[1]

[1]Technical University of Kosice, Faculty of Manufacturing Technologies with a seat in Presov, Slovakia

DOI: 10.17973/MMSJ.2024_12_2024112

radoslav.vandzura@tuke.sk

Presented paper is focused on the experimental welding of aluminium alloys – the additively manufactured material AlSi10Mg and the conventional alloy AW-5754. The experimental electron beam welding was conducted in collaboration with First welding company, Inc. The objective of the experiment was to create a weld joint between aluminium alloys prepared by additive and conventional methods, evaluate the base materials, the heat-affected zones (HAZ), and the weld joint in terms of microstructure, as well as measure and assess microhardness.

KEYWORDS

electron beam welding, additive manufacturing, AlSi10Mg, AW-5754

1 INTRODUCTION

Electron Beam Welding (EBW) is an advanced welding technology used to achieve high-quality weld joints, particularly in materials with high mechanical property demands. This technology utilizes a focused electron beam to perform welding in a vacuum chamber, which allows high precision, minimal thermal impact on the surrounding material, and reducing the risk of deformation and defects [Weglowski 2016]. EBW has proven to be highly effective in joining materials with different properties and is widely used in industries where high demands for mechanical properties and precision are required, such as in the aerospace and automotive sectors [Eakins 1998]. Currently, research on welding of additively manufactured materials is highly relevant. Additive manufacturing (AM) is becoming increasingly popular due to its ability to create complex geometric shapes and optimize material consumption [Riddick 2019]. The primary advantages of AM include increased geometric complexity, material savings, and the ability to produce parts with enhanced properties that are often difficult to achieve using traditional manufacturing methods [Davies 2020]. As additive technologies continue to advance, new opportunities arise for experiments in joining additively manufactured materials with conventional alloys, which presents challenges for welding technologies. Current research focuses on identifying and addressing challenges related to joining additively manufactured and conventional materials. Studies show that additively manufactured materials can exhibit different microstructural properties and mechanical characteristics compared to conventionally produced materials [Munro 2013]. These differences can affect the quality of the weld joint and require thorough analysis to ensure the integrity and performance of the welds. Additionally, optimizing welding parameters is crucial to overcome challenges posed by the distinct thermal and chemical properties of additive materials [Sundaram 2022]. For instance, studies on additively manufactured aluminum alloys indicate that these materials may have higher porosity and varied microstructural characteristics, which can influence the final quality of the weld joint [Harlow 2019]. Reversibly research focused on welding of additively manufactured components with conventional materials has revealed that precise control of welding parameters is key to achieving high-quality welds that meet mechanical properties and durability requirements [Fisher 2018].

These findings highlight the need for further research and optimization of welding technologies for additively manufactured (AM) materials to ensure their successful integration into a wide range of industrial applications. Work in this area is essential for the advancement of welding technology and the practical application of additive materials in the industry.

2 MATERIAL AND METHODS

In preparation for the electron beam welding experiments, rectangular specimens with precise dimensions of 60x20 mm, 3 mm in thickness were produced from the AlSi10Mg and AW-5754 alloys. The AlSi10Mg alloy, fabricated using additive manufacturing (AM), combines the strength and hardness required for high-performance applications, primarily due to the formation of Mg2Si precipitates that enhance its mechanical properties. This makes it a suitable material for applications demanding increased wear resistance and structural integrity [Silvestri 2020].

AW-5754, a conventionally manufactured alloy, was selected for comparison due to its excellent corrosion resistance and balance of strength and formability. This alloy is widely used in industries such as automotive and marine [Mucha 2021]. Comparing these two distinct alloys—one produced via AM and the other conventionally—will provide critical insights into the impact of different manufacturing techniques on the weldability and performance of aluminum alloys.

The chemical composition of the AlSi10Mg powder material used in AM, detailed in Table 1. [Renishaw 2023a], is essential in determining the final characteristics of the alloy. Detailed control of these compositions ensures that the specimens are consistent, enabling reliable comparisons in the subsequent welding and mechanical evaluations of microstructure, heat-affected zones, and hardness testing.

Table 1. Chemical composition of AlSi10Mg alloy powder material

Elements	w (%)	Elements	w (%)
Si	9–11	**Zn**	≤ 0.1
Fe	≤ 0.55	**Pb**	≤ 0.05
Cu	≤ 0.05	**Ti**	≤ 0.05
Mn	≤ 0.45	**Sn**	≤ 0.05
Mg	0.2-0.45	**Al**	rest.
Ni	≤ 0.55		

The experimental specimens were prepared using a Renishaw AM400 printer, a highly advanced machine designed specifically for precision additive manufacturing of metal components.

Renishaw AM400 utilizes selective laser melting (SLM) technology, a method that allows the creation of demanding metal parts layer by layer from metal powder by melting it with a focused laser. The AM400 is equipped with a 400 W fiber laser, which ensures high energy density and precise control during the melting process, making it ideal for the fabrication of complex geometries and high-strength materials [Renishaw 2023b].

The production of the experimental specimens was carried out in a controlled argon atmosphere to prevent oxidation during the melting process. This protective environment is crucial for maintaining the integrity and mechanical properties of the material, especially during working with sensitive aluminium alloys like AlSi10Mg. The Renishaw AM400 offers precise control over process parameters, including laser power, scan speed, and layer thickness, which contributes to achieving consistent material properties across the specimens. The arrangement of the specimens on the build platform was carefully planned to optimize the use of available space and ensure uniform cooling rates, which can influence the mechanical properties and microstructure of the final parts. Position of the specimen on the building platform is illustrated in Figure 1, which also highlights the strategic placement of support structures and orientation of the parts to minimize residual stresses and deformation during the printing process.

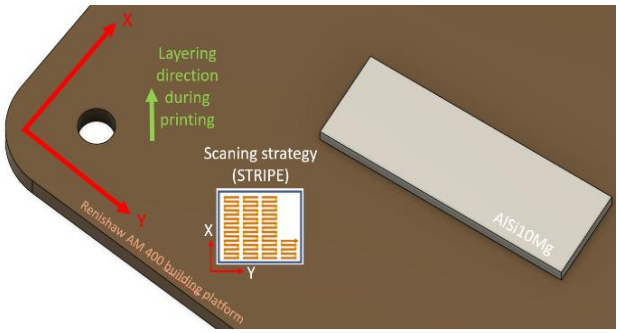

Figure 1. Orientation of the specimen on the building platform

Considering the dimensions of the experimental specimen, optimal parameters were chosen to prevent deformation of the specimen due to the influence of a heat and a high energy during the selective laser melting process. The printing process parameters for the specimens are listed in Table 2.

Table 2. Printing process parameters

Laser Power (P)	275 W
Scanning Velocity (v)	800 mm.s^{-1}
Layer Thickness (t_L)	30 µm
Part Thickness (t_P)	3 mm
Number of Layers (n_L)	100
Hatching distance (d)	80 µm

The total input energy of the laser beam ε= 143.23 J.mm^{-3}

$$\mathcal{E} = \frac{P}{v \cdot d \cdot t_L} \quad (1)$$

Where:

P - laser power 275 W, v - scanning velocity 800 mm.s^{-1}, t_L – layer thickness 30 µm, d- hatching distance 80 µm.

The scanning strategy for the laser movement was set to Stripe, which involves the laser tracing parallel lines across the powder bed in a sweeping motion (Figure 1).

The second base material is the aluminum alloy AW-5754. This aluminum alloy is primarily alloyed with magnesium. It is characterized by good mechanical properties, such as strength and toughness, and is highly processable and ductile. These properties make it suitable for applications where material lightness and resistance to mechanical wear are crucial. The chemical composition of the alloy is detailed in Table 3 [Thyssenkrupp 2021].

Table 3. Chemical composition of the alloy AW-5754

Elements	w (%)	Elements	w (%)
Si	≤ 0.4	**Cu**	≤ 0.1
Mg	2.6-3.6	**Zn**	≤ 0.2
Mn	0.5-1.0	**Ti**	≤ 0.15
Fe	≤ 0.4	**Al**	rest.

Welding of conventionally produced AW-5754 and additively manufactured AlSi10Mg material specimens was carried out using the Electron Beam Welding (EBW) complex EBW PZ ELZA UNI 2G, in collaboration with First welding company, Inc. (Slovakia, Bratislava). The welding machine is used for automated welding of materials in a vacuum chamber, either individually or in small batches. The machine includes an energy block with pulse power regulation, ensuring high stability of welding parameters. The welding process is fully automated and controlled by a control system [PZVAR 2023].

The aim of the experiment was to create a weld joint using this advanced welding method and to subsequently evaluate the weld joint. The welding parameters were fine-tuned and set as follows: Accelerating Voltage (U) = 55 kV, Welding Current (I_z) = 40 mA, Welding Speed (v_z) = 50 mm s^{-1}, Focusing Current (I_f) = 822 mA, Deflection = Circle D = approx. 1 mm, f = 555 Hz. The experimental weld specimen is shown in Figure 2.

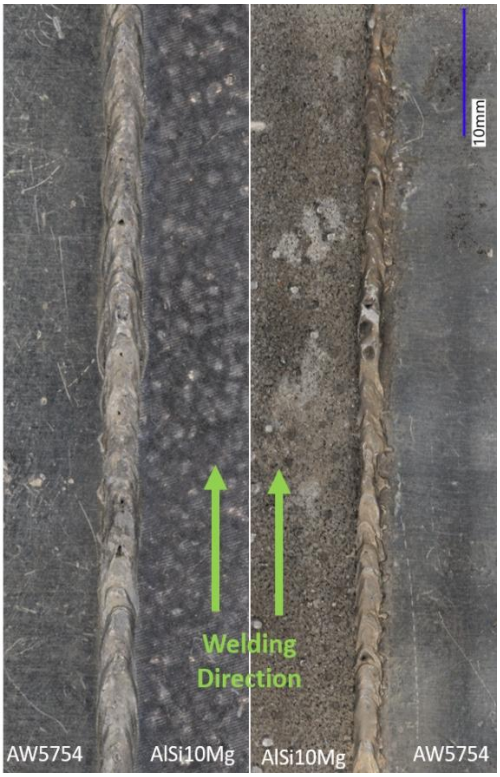

Figure 2. Weld joint: face side (left), root side (right)

3 RESULTS AND DISCUSION

After the welding process, the welded specimens underwent a comprehensive evaluation to thoroughly analyze the microstructural changes in the base materials, the weld joint, and the heat-affected zone (HAZ). The microstructural analysis was conducted to identify variations in phase distribution, and potential defects or inclusions within the weld and surrounding areas. Further assessment of the weld joint included

microhardness measurement to determine the mechanical properties across different zones. The surface morphology of the weld seam was evaluated using advanced 3D surface scanning technology. This 3D analysis provided detailed insight into the topographical changes, and potential deformations or irregularities resulting from the welding process, offering a deeper understanding of the weld integrity and quality.

3.1 3D optical analysis of the weld joint

Optical 3D surface scanning of the weld was performed using the Keyence VHX 7000 microscope, which enabled a detailed visualization of the surface morphology of the weld seam. The scan provides a detailed 3D profile analysis of the weld joint. In the images (Figure 3 and 4), a colour scale is applied to indicate height differences on the weld surface, with the range varying from 0.000 mm (blue) to 1.559 mm (red).

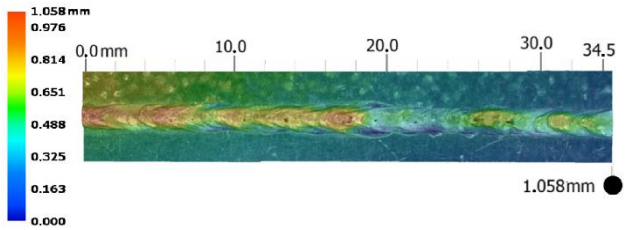

Figure 3. Morphology of the weld face surface

Figure 3 shows a 3D scan morphology of the weld face seam. The surface elevation of the weld exhibits irregularities, indicating non-homogeneous flow and solidification of the molten metal during the welding process. Porosity was observed to a small extent across the width of the weld joint. The elevation of the weld ranged from 0.2 mm to a maximum of 1.6 mm. The width of the weld varied from 1.322 mm to 1.540 mm.

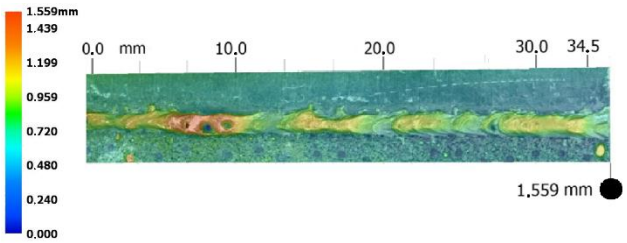

Figure 4. Morphology of the root weld surface

The morphology of the weld root (Figure 4) shows significant local height variations. These areas may indicate potential quality issues with the weld joint and the presence of defects such as porosity. In the right part of the weld root (20 to 35 mm), the surface morphology of the weld is more stable, which may suggest a more uniform melting and cooling process. Throughout the length of the weld, height variations range from 0.415 to 1.559 mm, while the width of the weld root ranges from 0.956 mm to 0.983 mm.

3.2 Microstructural analysis of the base material, HAZ, weld joint

For microscopic and macroscopic observation, a metallographic specimen was prepared using the standard method of embedding the specimen in resin, grinding underwater with sandpapers from P180 to P4000, polishing on cloth with abrasive microparticles of 0.1 µm, and subsequently etching the surface to enhance the resulting structure with Barker's etchant. Images for microstructural observation were captured using a Nikon MA100 optical microscope.

In the macro image of the weld joint (Figure 5), different areas can be observed between the base materials, the heat-affected zone (HAZ), and the weld metal itself. The base material AlSi10Mg exhibits a fine structure and increased porosity toward the weld metal. The pores in this area are likely a result of rapid cooling and inhomogeneity during welding.

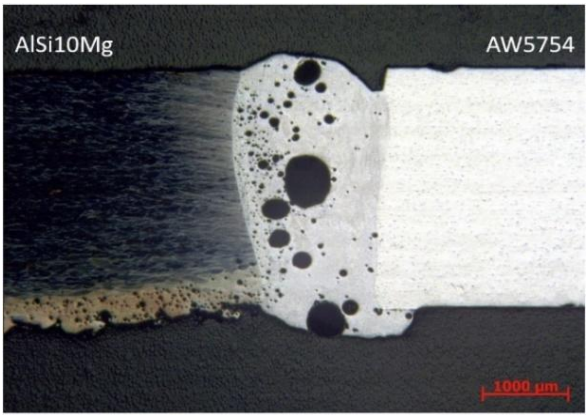

Figure 5. Weld joint in section

Pores at the bottom of the material are related to its preparation method, particularly from the support structures connecting the printed material to the print bed. The conventional material AW-5754 shows a more homogeneous structure without defects, indicating a more stable material state without significant flaws. The weld metal (the central part of the image) contains visible porosity defects, which may be caused by the welding process, insufficient gas venting during cooling, or the properties of the AM material and its specific characteristics concerning the specimen dimensions and printing parameters. These pores can negatively impact the strength and integrity of the weld joint. The heat-affected zone (HAZ) at the interface between the base materials and the weld exhibits significant transitions in microstructure, caused by thermal stresses during welding. Fine structures and micro-defects may form in this area, affecting the mechanical properties of the joint.

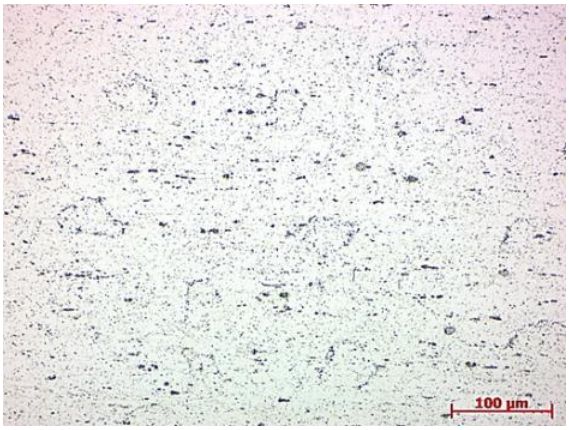

Figure 6. Microstructure of base material AW-5754, magnification 100x

The base material of the conventional alloy AW-5754 (Figure 6) has a polyhedral grain morphology. From a macroscopic perspective, there is no porosity or discontinuity in the material's structure, confirming a high-quality metallurgical process in the production of the material production. The microstructure consists of the α phase (Al), which is a solid solution of magnesium in aluminium. The structure also includes Mg_2Al_3 phases with varying morphologies that formed as precipitated particles during the cooling and processing of the alloy.

The base material AlSi10Mg produced additively (Figure 7) is characterized by a specific spherical substructure that is morphologically oriented along the vector of the laser movement during the powder material sintering process. The microstructure of individual cells is dendritic, delineated by clearly visible arc-shaped geometries of the segregates at the

boundaries of the imaginary grains. Upon reviewing the SLM layer formation methodology, very minimal intercellular discontinuity and pronounced substructural porosity or cavities are observed. Imperfectly melted AlSi10Mg powder particles are not detected.

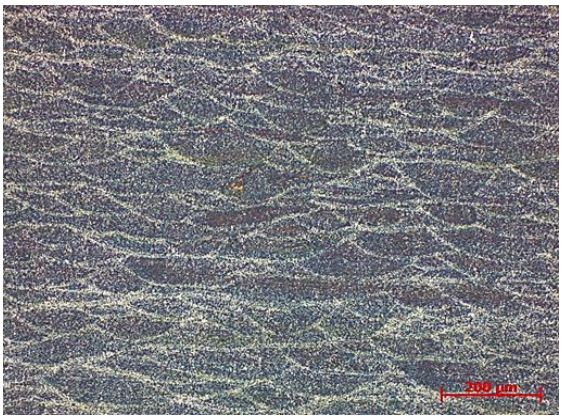

Figure 7. Microstructure of base material AlSi10Mg, magnification 50x

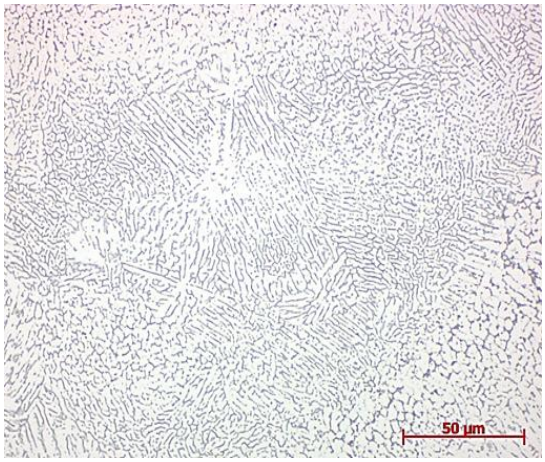

Figure 8. Microstructure of weld joint, magnification 250x

The structure of the weld joint (Figure 8) is composed of dendrites of the α-Al phase, which is a causal result of primary crystallization due to the rapid heat extraction from the area. Interdendritic segregates of minor phase composition are distinctly observed, defined by the chemical composition of the intermetallic phases β-Si and Mg.

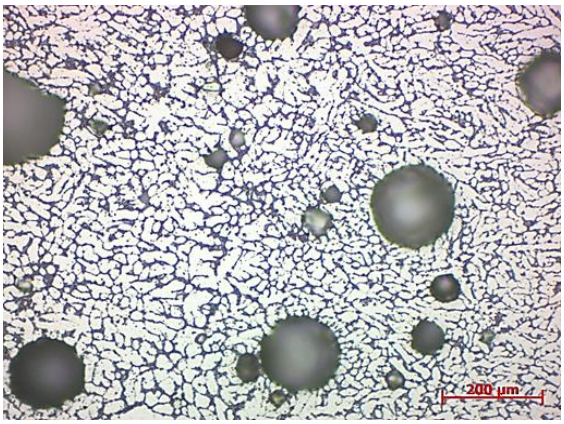

Figure 9. Microstructure of weld joint, magnification 50x

From a macroscopic view in magnification 50x (Figure 9), of the weld metal shows significant porosity of separate cavities, which results from the set parameters of the welding technological process and the properties of the alloy.

In the heat-affected zone (HAZ) on the side of the base material produced by SLM (Figure 10), a gradual disappearance of distinct structural boundaries between individual cells is visible. This phenomenon is observed moving from the melting boundary into the unaffected part of the base material.

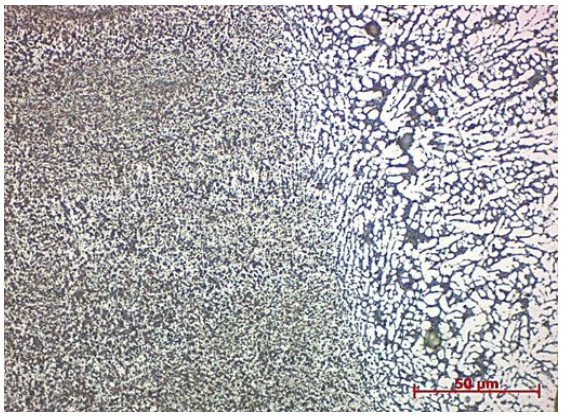

Figure 10. Microstructure of HAZ AlSi10Mg, magnification 250x

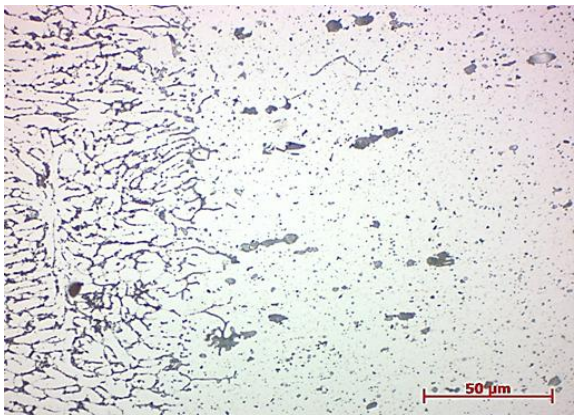

Figure 11. Microstructure of HAZ AW-5754, magnification 250x

On the HAZ side of the alloy produced by conventional methods in the heat-affected zone, where recrystallization of the α-Al matrix occurs, no morphological or structural changes in the phase composition of the alloy are observed (Figure 11). From the perspective of image analysis, the mixing of the weld metal with the base material is sufficient, showing a smooth structural transition between the different areas of the joint.

3.3 Measurement and analysis of microhardness of the weld joint

Measurement of Vickers microhardness was conducted using the CV-400 DAT Vickers Microhardness tester. Microhardness measurement was performed on the base materials, the heat-affected zones (HAZ), and the weld joint.

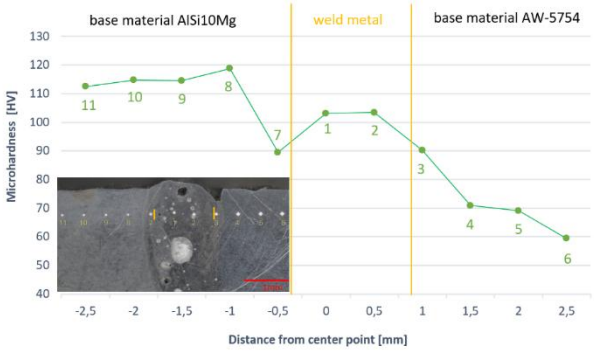

Figure 12. Measuring of microhardness

Microhardness measuring (Figure 12) in the weld joint shows significant variations depending on the area. In the base material AlSi10Mg, the microhardness is the highest, ranging from 110 to 120 HV, and remains relatively stable. In the heat-affected zone (HAZ) near the AlSi10Mg, the microhardness decreases to

around 90 HV, indicating a marked decrease due to thermal stress during welding. In the weld metal itself, microhardness reaches values between 100 and 110 HV. On the HAZ side near the conventional material AW-5754, the microhardness slightly increases to about 90 HV but remains lower than in the base material AlSi10Mg. The base material AW-5754 exhibits the lowest microhardness values in the entire weld joint, approximately between 60 and 70 HV.

CONCLUSIONS

Presented study demonstrated the feasibility of electron beam welding (EBW) for joining additively manufactured aluminium alloy AlSi10Mg and conventionally processed AW-5754. The results showed that the additively manufactured AlSi10Mg exhibited higher porosity and localized structural defects, probably caused by rapid cooling and the characteristics of the additive manufacturing process. In contrast, the conventional AW-5754 alloy displayed better microstructural stability and fewer defects.

Surface analysis revealed height variations from 0.2 mm to 1.6 mm on the weld face and from 0.415 mm to 1.559 mm in the weld root. Microstructural analysis indicated dendritic α-Al structures in the weld, with significant changes in the heat-affected zone (HAZ) on the AlSi10Mg side, but minimal changes on the AW-5754 side.

Microhardness testing showed higher values in AlSi10Mg (110 – 120 HV) compared to AW-5754 (60-70 HV), with the hardness in the weld metal (100 – 110 HV).

Morphological and microstructural analyses highlight the importance of controlling process conditions to minimize defects and improve overall joint integrity. Further research aimed at optimization of welding parameters and process techniques is recommended to improve the quality and reliability of the welds.

Overall, while EBW is a suitable method for joining these materials, weld quality depends on optimized welding parameters and material preparation.

ACKNOWLEDGMENTS

This publication is the result of the Project implementation: Automation and robotization for 21st century manufacturing processes, ITMS: 313011T566, supported by the Operational Programme Research and Innovation funded by the ERDF;

KEGA 017TUKE-4/2023: Implementation of research findings of additive production technologies into study programs of FMT TUKE;

VEGA 1/0391/22: Research and application of new technological procedures of nondestructive testing of additive manufacturing products;

APVV-21-0228Research of welded joints properties of metal components prodeced by additive technologies SLM and SLS.

REFERENCES

[Davies 2020] Davies, M. J. Advances in Additive Manufacturing: A Review. Materials Science and Engineering, 2020, Vol. 780, pp. 284-292.

[Eakins 1998] Eakins, D.S. Electron Beam Welding: Theory and Applications. Journal of Materials Processing Technology, 1998, Vol. 73, No. 1-3, pp. 53-63.

[Fisher 2018] Fisher, L.Z. Electron Beam Welding of Conventional and Additive Manufactured Materials. Welding Journal, 2018, Vol. 97, No. 7, pp. 245-253.

[Harlow 2019] Harlow, R.B. Microstructural Characteristics of Additively Manufactured Al-Si-Mg Alloys. Materials Characterization, 2019, Vol. 60, No. 1, pp. 15-24.

[Mucha 2021] Mucha, J., Kascak, L., Witkowski, W. Research on the influence of the AW 5754 aluminum alloy state condition and sheet arrangements with AW 6082 aluminum alloy on the forming process and strength of the ClinchRivet joints. Materials, 2021, Vol. 14, No. 11, p. 2980.

[Munro 2013] Munro, A.M., et al. Comparative Study of Additive Manufacturing and Conventional Materials. International Journal of Machine Tools and Manufacture, 2013, Vol. 72, pp. 1-11.

[PZVAR 2023] PZVAR. Technological Complexes for Electron Beam Welding [online]. 2023. Available from https://www.pzvar.sk/en/produkty/zvaracie-zariadenia-automatizovane-komplexy/technological-complexes-electron-beam-welding.

[Renishaw 2023a] Renishaw. RENAM 500 Series Aluminium AlSi10Mg Material Data Sheet [online]. 2023. Available from https://www.renishaw.com/resourcecentre/download/data-sheet-renam-500-series-aluminium-alsi10mg-material-data-sheet--130331.

[Renishaw 2023b] Renishaw. Venturing into metal additive manufacturing [online]. 2023. Available from https://www.renishaw.com/en/venturing-into-metal-additive-manufacturing--44511.

[Riddick 2019] Riddick, A.T. Additive Manufacturing: Technologies and Applications. Advanced Manufacturing Technology, 2019, Vol. 22, No. 4, pp. 289-305.

[Silvestri 2020] Silvestri, A.T., et al. Assessment of the mechanical properties of AlSi10Mg parts produced through selective laser melting under different conditions. Procedia Manufacturing, 2020, Vol. 47, pp. 1058-1064.

[Smith 2001] Smith, D., et al. Specification Formulation. Journal of Engineering, 2001, Vol. 2, No. 2., pp. 223-228. ISSN 0954-4828.

[Sundaram 2022] Sundaram, S.S. Optimizing Electron Beam Welding for Additive Manufactured Materials. Journal of Manufacturing Processes, 2022, Vol. 45, pp. 344-355.

[Thyssenkrupp 2021] Thyssenkrupp. AW 5754 Aluminium Alloy Data Sheet [online]. 2021. Available from https://ucpcdn.thyssenkrupp.com/_legacy/UCPthyssenkruppBAMXUK/assets.files/material-data-sheets/aluminium/5754.pdf.

[Weglowski 2016] Weglowski, M.S., Blacha, S., Phillips, A. Electron beam welding – Techniques and trends – Review. Vacuum, 2016, Vol. 130, pp. 72-92.

CONTACTS:

Eng. MSc. Radoslav Vandzura, PhD.
Technical University of Kosice, Faculty of Manufacturing Technologies with a seat in Presov
Bayerova 1, 080 01 Presov, Slovakia
radoslav.vandzura@tuke.sk